



THE GEOLOGIC CONTEXT OF WONDERSTONE: A COMPLEX, OUTCROP-SCALED PATTERN OF IRON-OXIDE CEMENT

DEREK T. BURGESS, RICHARD M. KETTLER, AND DAVID B. LOOPE
Earth & Atmospheric Sciences, University of Nebraska, Lincoln, Nebraska 68588, U.S.A.

ABSTRACT: Although siderite is a widespread early diagenetic mineral in fluvial systems, it is unstable in oxidizing environments and destroyed in permeable rocks that experience uplift and exhumation. The products of siderite oxidation, however, (mm- to cm-scale rhombs, concretions, and complex bands of iron-oxide cement) are widespread in the rock record of fluvial systems. The fluvial channels of the Shinarump Member of the Chinle Formation in southern Utah and northern Arizona, U.S.A., provide an excellent suite of examples of diagenetic features produced by Triassic and Neogene oxidation of early diagenetic siderite. These diagenetic features also provide direct evidence of the level of the water table during deposition of the Shinarump member.

Large, *in situ*, discoidal concretions containing preserved siderite are present in Shinarump floodplain siltstones. Rip-up clasts derived from the siltstones developed iron-oxide rinds during late-stage, near-surface oxidation. These two structures show that floodplain silts contained abundant organic matter and methanic pore water. Groundwater recharging through these silts carried reducing water through underlying sand bodies and discharged into active channels. Degassing of CO₂ and methanogenesis caused rhombic crystals of siderite to precipitate in channel sands during these wet intervals. Some of this siderite may have been oxidized during dry intervals when groundwater circulation reversed, but most siderite in the channel sands was preserved until the Shinarump was exhumed during the Neogene.

As oxygenated near-surface water entered joints in the lithified Shinarump, colonies of iron-oxidizing microbes living in the phreatic zone occupied redox boundaries and used the rhombic crystals of siderite in the sandstone and the spherulitic siderite in transported siltstone intraclasts as their sources of energy and carbon. The ferrous iron released from dissolving siderite within the intraclasts was oxidized at the siltstone–sandstone contact, generating rinded concretions similar to those in the Cretaceous Dakota Formation. Complex banding known as wonderstone was produced in the channel sandstones from oxidation of the rhombic siderite; the pattern is a combination of Liesegang bands and microbially mediated cements. The preserved rhombs are pseudomorphs after siderite crystals that were either oxidized during Triassic dry intervals, or escaped Neogene microbial oxidation in the phreatic zone, only to be oxidized abiotically in the vadose zone. Microbes are likely oxidizing Shinarump siderite a few kilometers down dip of outcrops with exposed wonderstone. At such locations, the Shinarump is in contact with overlying water-saturated Quaternary alluvium.

INTRODUCTION

Ever since the Great Oxidation Event near the close of the Archaean (stage 6 of Hazen et al. 2008), siderite (FeCO₃), though still a relatively abundant mineral, has been banished to the subsurface. In areas undergoing exhumation, the products of siderite oxidation should be abundant, but until recently, sedimentologists and geomicrobiologists have paid scant attention to the alteration products of siderite.

Although ancient fluvial and eolian sandstones are commonly red (Walker 1974; Walker et al. 1978), reducing fluids can dissolve and mobilize the ferric iron in their grain coatings as Fe⁺⁺. Much of this ferrous iron is likely to be precipitated as ferrous carbonate (siderite or ankerite; Loope et al. 2010; Loope and Kettler 2015). These carbonates will be oxidized when their host rock is invaded by near-surface, meteoric water. This oxidation can take place while the sedimentary matrix is still in its

depositional environment, or, as in most of the examples discussed here, it can occur after lithification, many millions of years after deposition.

The motivation for this study is to better understand the geologic context of the pattern of colorful bands (Fig. 1) that develops during the diagenesis of a wide variety of porous and permeable rocks. The pattern is composed of alternating iron-oxide stains and dense, mm- to cm-scale cement bands that most geologists referred to as “Liesegang banding” (Kettler et al. 2015). Dissolution and oxidation of siderite commonly involves cm-scale transport of Fe⁺⁺ in an aquifer, and results in rind-like cements of microbial origin (Weber et al. 2012; Kettler et al. 2015). This paper describes the various iron-rich diagenetic structures in the Shinarump Member of the Chinle Formation and attempts to decipher the dynamics of groundwater flow in the Triassic depositional system, as well as the timing and sequence of diagenetic events recorded by the sandstones and siltstones seen today.

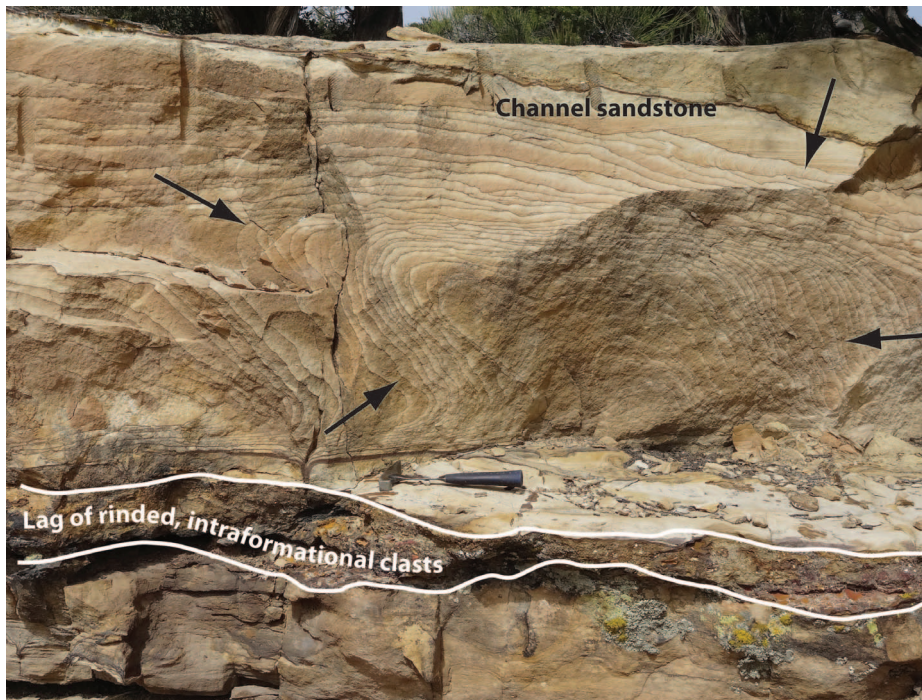


FIG. 1.—Wonderstone exposed in road cut on Lost Spring Mountain, Utah. Primary sedimentary structures are not visible in the channel sandstone. Black arrows show inward progression of oxidation fronts as disseminated siderite crystals were dissolved and iron-oxide-cemented bands were precipitated by microbial colonies. Intraformational clasts composed of sideritic floodplain siltstone were eroded, transported, and deposited by Late Triassic streams; their iron-oxide rinds and the Wonderstone patterns did not form until Shinarump strata were exhumed and oxidized during the Neogene.

Large, partially oxidized siderite concretions encased within floodplain siltstones and iron-oxide-rinded intraformational clasts provide evidence for the development of reducing pore waters during Shinarump deposition. In addition, laterally extensive, channel sandstone bodies contain: 1) disseminated, rhombic pseudomorphs composed of iron oxide; and 2) the complex pattern that Kettler et al. (2015) called “wonderstone.” Both phenomena are alteration products of early diagenetic siderite: siderite crystals that were oxidized *in situ* are now preserved as rhombic pseudomorphs, and the wonderstone pattern formed when complete dissolution of siderite was followed by cm-scale migration of ferrous iron toward redox boundaries populated by iron-oxidizing microbes.

GEOLOGIC SETTING

The study areas (Fig. 2) lie along the border between northwestern Arizona and southwestern Utah, U.S.A. Most fieldwork was performed along the Chocolate Cliffs near the town of Colorado City, Arizona. The Shinarump Member of the Chinle Formation (Fig. 2) was deposited on an erosional surface in a back-arc basin that formed during the Sonoma orogeny when an island-arc system accreted along the western edge of Pangea (Dickinson 1981). The Chinle Basin drainage extended from the craton (western Texas) to the edge of the supercontinent (Arizona, Utah, and Nevada; Dickinson and Gehrels 2008). The fluvial Shinarump Member is the lowest stratigraphic unit of the Chinle Formation (Fig. 2C), and overlies the Tr-3 unconformity, which separates the Upper Triassic Chinle Formation from the Middle and Lower Triassic Moenkopi Formation.

Fluvial, fining-up channel sandstones in the multi-story, cliff-forming Shinarump Member are separated by thin siltstones (Fig. 3). In the study area, the Shinarump is composed dominantly of fine to coarse sandstones and locally includes pebble conglomerate. It varies in mineralogical maturity from quartz arenite to quartzose volcanic wacke (Stewart et al. 1972). Conglomerate clasts are mostly extraformational and dominantly comprise chert, quartz, and quartzite clasts. Iron-oxide-rinded intraclasts (see below) are less abundant. Shinarump channel sandstone deposits are cross-stratified, structureless, or horizontally bedded (Stewart et al. 1972; Blakey and Gubitosa 1983). These fluvial deposits comprise a thin,

discontinuous sheet that filled paleovalleys incised into the Moenkopi Formation; they comprise a lowstand systems tract (Beer 2005). Stewart et al. (1972) considered the Shinarump sandstones as channel-lag and point-bar deposits, and the siltstones as floodplain accumulations. As base level rose and incised valleys were filled, streams migrated laterally between valley walls, producing abundant lateral-accretion surfaces (Blakey and Gubitosa 1983; Dubiel 1992; Dubiel and Hasiotis 2011).

Paleosols in the Chinle Formation vary from waterlogged, kaolinitic Oxisols and Gleysols at the base (Shinarump and equivalents) to well-drained Calcisols and Aridisols in the upper members (Dubiel and Hasiotis 2011). This trend has been attributed to a long-term decline in precipitation that coincided with diminishing precipitation when what is now western North America moved northward from the wet tropics and through Pangea’s northern monsoon belt (Prochnow et al. 2006; Dubiel and Hasiotis 2011; Atchley et al. 2013).

PREVIOUS STUDIES

According to Berner’s (1981) classification, diagenetic siderite forms in sediments that are anoxic, nonsulfidic, and methanic. Siderite is typically (but not exclusively) associated with nonmarine strata (carbonate \gg sulfate; Berner 1981; Pye et al. 1990). Mineral assemblages change as groundwater chemistry changes. In particular, reduced-iron minerals are unstable in aerobic conditions, and become oxidized, producing secondary ferric minerals. Although iron transport is limited, except in strongly acidic waters or reduced waters, reducing waters are capable of producing copious amounts of ferrous mineral cements. Because these ferrous cements are easily oxidized, iron-oxide cements and concretions likely had ferrous (reduced) iron precursors (Curtis and Coleman 1986). Recognizing an iron-bearing mineral as secondary and linking its presence to the oxidation of a particular precursor mineral thus is essential to understand the evolution of pore-water chemistry. Spherical concretions from the Jurassic Navajo Sandstone that have external rinds cemented by iron-oxide and iron-poor cores have been recently identified as products of changing redox conditions during late diagenesis (Loope et al. 2010, 2011; Loope and Kettler, 2015; Kettler et al. 2012; Weber et al. 2012). In the Navajo

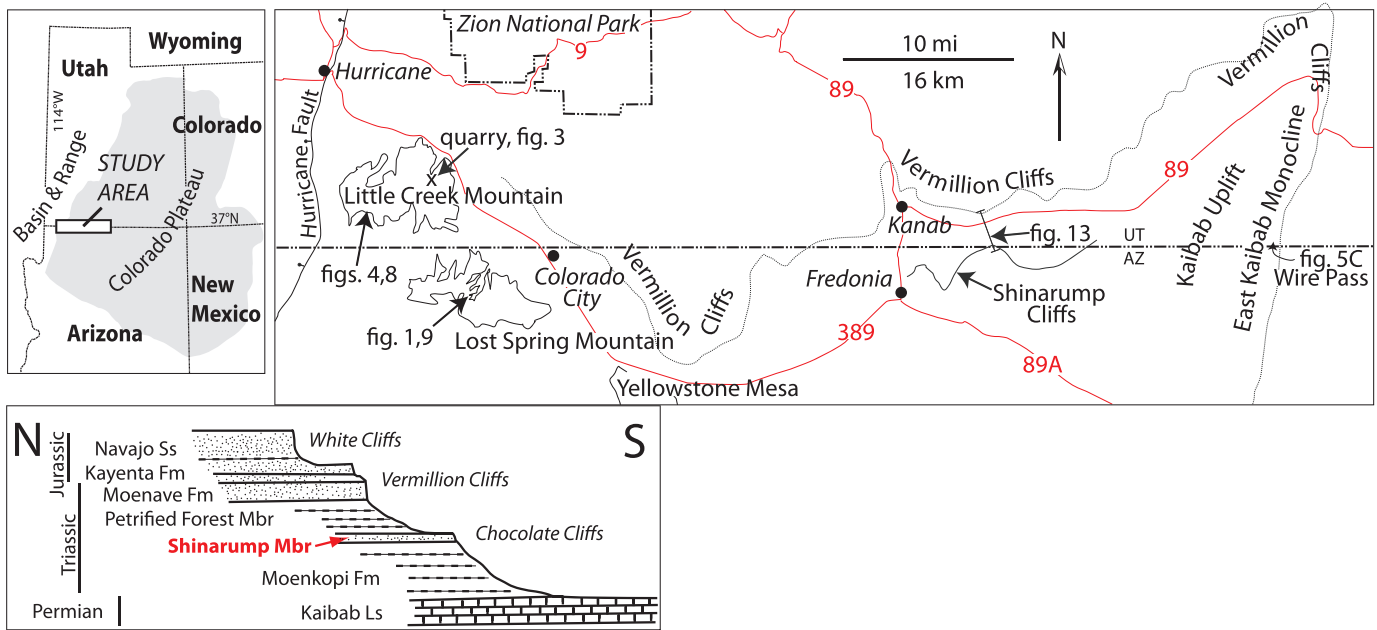


FIG. 2.—A, B) Locations of study areas and C) generalized stratigraphic section.

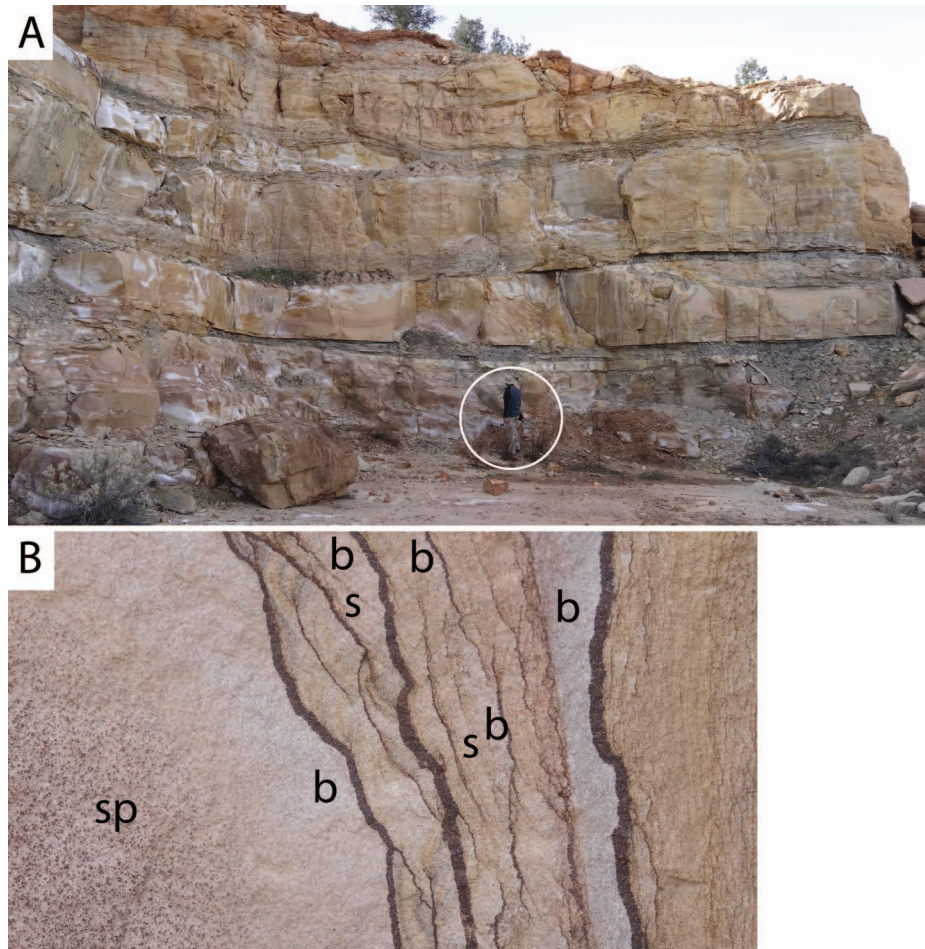


FIG. 3.—Shinarump strata exposed at an abandoned wonderstone quarry, Little Creek Mountain, Utah. A) Quarry walls show multi-story sandstones with thin intervening siltstones; geologist for scale (in circle). B) Close-up of wonderstone with distinct, dark bands cemented by iron-oxide cement. Bands are convex toward the left (direction of migration of redox boundaries). Colored zones with faint striping that lie between the dark bands comprise stains (s), which are interpreted as Liesegang bands (Kettler et al. 2015). In bleached zones (b), the reducing fluid dissolved the stain. The speckled area to left (sp) contained disseminated siderite crystals that are now preserved as iron-oxide pseudomorphs after siderite. Disseminated siderite crystals were the source of iron (for energy) and carbon (for biomass) for microbial colonies that precipitated the oxide-cemented, dark bands to the right. Pseudomorphs occupy the former locations of ferrous carbonate crystals that were not dissolved and metabolized by the microbial colonies; the ferrous iron that was dissolved and metabolized became the ferric iron cement bands—the waste products of the colonies.

Sandstone, late diagenetic, reducing pore-water flowed through anticlines charged with CO₂ and CH₄ and mobilized ferric iron from iron-oxide coatings on quartz grains (Beitler et al. 2003; Loope et al. 2010). Groundwater flowed down gradient from anticlines and precipitated siderite, forming concretions of varied shapes and sizes. No siderite is preserved in Navajo concretions, but abundant rhombic, iron-oxide pseudomorphs after siderite are present in the centers of large (meter-scale) concretions that are bounded by dense, iron-oxide rinds. The pseudomorphs are evidence that siderite crystals cemented the precursor concretion, and (during oxidation) were the source of ferrous iron for the rinds (Loope et al. 2011, 2015). Although ferroan calcite, ferroan dolomite, ankerite, and siderite can form rhomb-shaped euhedra, mass balance calculations for Navajo spheroidal concretions favor siderite as the original (precursor) cement (Loope et al. 2010).

Van der Burg (1969, 1970) studied rinded mud clasts in fluvial Pleistocene sand and gravel deposits of the Netherlands. He showed that iron-oxide rinds develop in the outermost portions of the mud clasts and grow inward. The source of iron was mm-scale spherosiderite nodules that displaced sediment as they grew radially in floodplain mud. Eventual dissolution of the siderite in the mud clasts generated voids; hence the hard, rinded concretions are “rattle stones.” Rattle stones are abundant in outcrops of the Cretaceous Dakota Formation in southeast Nebraska (Loope et al. 2012), and siderite is preserved in subsurface Dakota paleosols (as spheroidal nodules with radial structure) and in channel sandstones (as large, rhombic crystals; Ludvigson et al. 1996). Witzke and Ludvigson (1994) also reported abundant Liesegang banding from Dakota outcrops in eastern Iowa. Kettler et al. (2015) established that the iron-oxide cementation pattern locally called wonderstone (Fig. 1) is the product of microbial oxidation of siderite and apparent abiotic oxidation of adsorbed ferrous iron. Wonderstone is quarried from the channel-sandstone facies of the Shinarump Member in southwestern Utah and northwestern Arizona.

DESCRIPTION OF IRON-RICH STRUCTURES IN THE SHINARUMP MEMBER

Shinarump siltstones, sandstones, and pebble conglomerates contain a wide variety of iron-rich structures. Siltstones are generally thin and blocky; those at Little Creek Mountain are thinly laminated. Sandstones in the study areas have erosional bases and fine upward. Large-scale trough crossbedding near the base of sand bodies gives way to ripple-laminated strata at the top, but structureless sandstones are also common. All the sandstones are light-colored; detrital grains generally lack iron-oxide coatings.

Large Discoidal Concretions in Siltstone

These massive concretions are present in thin-laminated siltstones that directly overlie current-rippled sandstone in fining-up sequences. The siltstones form gentle, recessive slopes between the more-resistant sandstone units. The horizontal laminae are of millimeter scale and composed of silt- to clay-size grains. Intact concretions (Fig. 4), can be excavated from hillslopes littered with curved, cm-scale shards of shattered concretions. The largest discoids reach ~ 50 cm in diameter and masses of ~ 55 kg. Bedding is faintly visible in some concretions and is overprinted with iron-oxide cement. In thin sections, silt-size detrital grains can be seen to “float” in an iron-oxide matrix. QemScan shows the concretions to be dominated by reduced-carbonate minerals including siderite, rhodochrosite, and ankerite (46%), barite (20%), calcite (10%), and minor amounts of iron oxide (4%), and pyrite (3%) (Burgess 2014). Cements and internal cracks (septaria) are present throughout these concretions, and concretion centers are poorly cemented relative to the outer portions. Barite is restricted to fracture fills and appears to replace calcite crystals. Septaria both predate and crosscut other cements. Dendrites composed of iron-oxide cement are arranged along fractures, and others are present along bands near the concretion perimeter (Burgess 2014).

Disseminated Iron-Oxide Rhombs in Sandstone

These structures (Fig. 5) are mm- to cm-scale accumulations of iron-oxide cement. They are abundant in many Shinarump outcrops, as well as in the cores found in abandoned wonderstone quarries. Dark rhombs that are only partially filled by iron oxide are also present in some outcrops. In structureless sandstones, the rhombs are evenly distributed and similar in size; in stratified rocks, rhombs in coarser strata are larger and more abundant than those in finer-grained strata. Rhombs are also present in the cores of some tabular concretions (see below). At one site, rhombs preferentially cement cross bedded sandstone that surrounds large, cylindrical structures that reach 25 cm in diameter and lengths up to 10 m (Fig. 6A). Cylinder centers are composed of loose-packed, uncemented sand or are voids. The long axes of these structures lie parallel to the dip direction of surrounding trough cross-strata (Fig. 6A).

Wonderstone Pattern in Sandstone

The wonderstone pattern (Fig. 1, 7) comprises two iron-rich elements: cement bands and stain (Kettler et al. 2015). The area between cement bands regularly varies between lightly stained rock and rock lacking iron-oxide staining (Kettler et al. 2015). Iron-oxide staining bands are arcuate, and they abut the bands of iron-oxide cement. Both cement and staining bands crosscut and conceal sedimentary structures (Fig. 1), but the distributions of both these diagenetic structures are controlled by vertical joints that cut the sandstone at regular intervals.

On a larger scale, wonderstone displays two distinct patterns. Type 1 patterns are present only in jointed rock; multiple, concentric cement bands are arranged subparallel to the perimeters of blocks defined by joints and master bedding planes. In three dimensions, scallops are convex toward the centers of the blocks (Fig. 1B). In Type 2 patterns, joints (if present) crosscut cement bands. In vertical cross sections, cement bands can be concentric (Fig. 7) or nearly parallel, but in concentric patterns, scallops are always convex outward.

Pyrite Concretions in Sandstone

Spherical to ovoid pyrite concretions are present within both ripple-laminated and cross bedded sandstone, and they have a grain-supported fabric. These concretions are orange to yellow in color, and unoxidized pyrite is present in many. A few are nearly completely hollow; their former positions are marked by iron-oxide stain that forms long, vertical streaks on cliff faces (Fig. 6B).

Tabular, Jointed Iron-Oxide Concretions in Sandstone

These concretions are present only at the Little Creek Mountain site. They are cemented by iron oxide that precipitated along multiple intersecting sets of joints that cut current-rippled sandstones. Tabular concretions (Fig. 8A, B) formed in the uppermost portion of current-rippled sandstone bodies, in contact with laminated siltstone. Ovoid concretions formed as much as one meter below this contact. Joints trend NNW, N, and ENE (Fig. 8C); the ENE-trending joints always terminate at NNW- and N-trending joints, and most NNW-trending joints terminate at N-trending joints. Field measurements as well as Google Earth observations indicate that joints in box-work concretions at Little Creek Mountain are parallel to adjacent uncemented fractures.

Pore-filling iron oxide forms vertical rinds up to 1 cm thick; rinds project about 10 cm into the sandstone. In a typical plan view, rinds abut both sides of open, hairline fractures, and light-colored, iron-poor sandstone occupies the central portion of each joint-bounded polygon. Some central portions contain disseminated, iron-oxide pseudomorphs. No rind is present along the contact with the overlying siltstone. In a distinct variant of these concretions, rinds are U-shaped in vertical cross section



FIG. 4.—Large, discoidal concretions in floodplain siltstones, Little Creek Mountain. **A)** *In situ* concretion (black arrow); note lamination of siltstone. **B)** Shattered remains of discoidal concretions on modern hill slope (cf. Fig. 10). Curved fragments are from perimeters of large discoids. **C)** Cross-sectional view of large, discoidal concretion. Calcite (white) fills septarian fractures. Note bands of iron-oxide cement along the perimeter (white arrows).

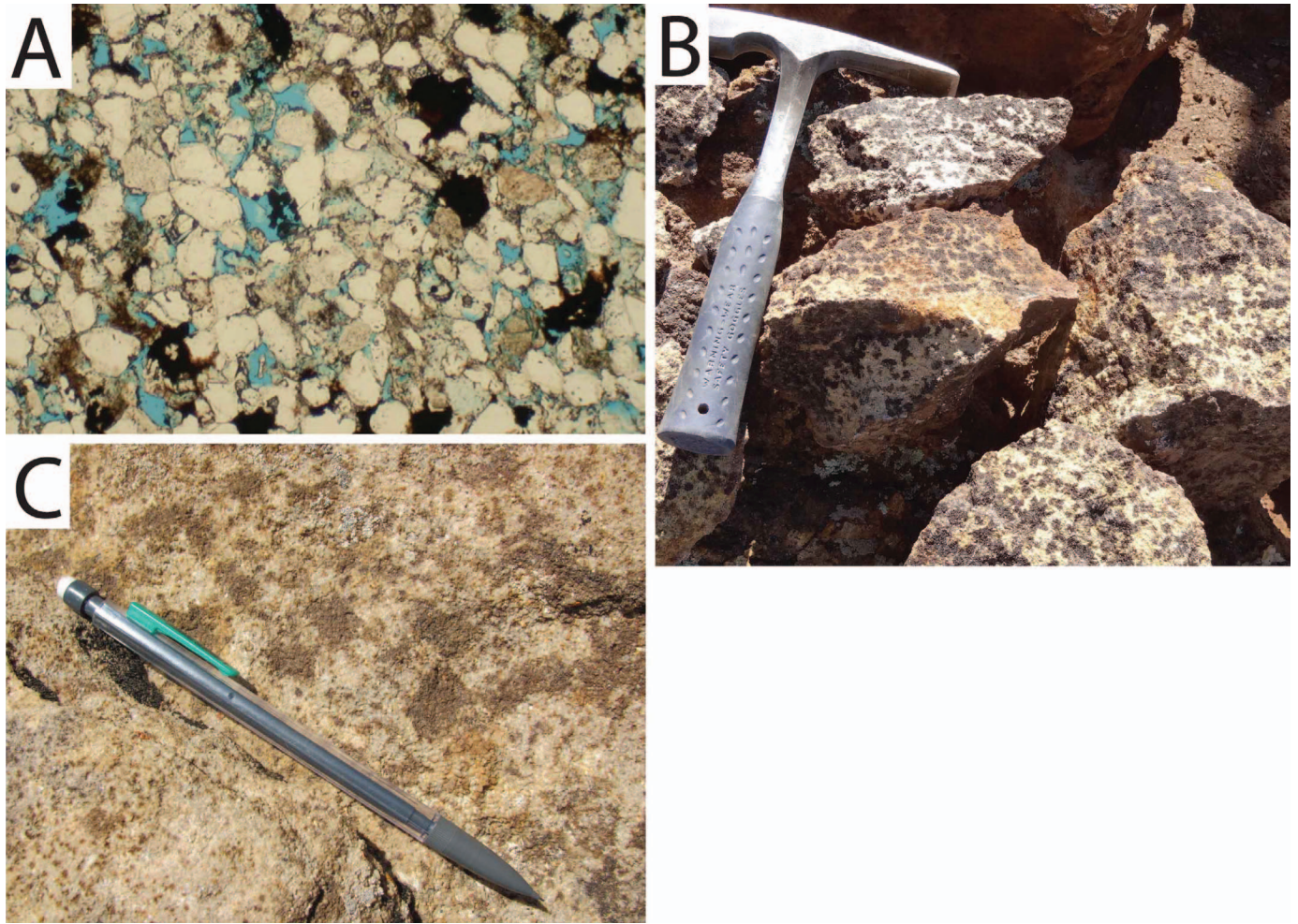


FIG. 5.—Rhombic cement crystals. **A)** Thin section, plane light; **B)** outcrop, Wire Pass; **C)** outcrop, Little Creek Mountain.

(Fig. 8B). In these, sandstone with disseminated pseudomorphs (rather than dense rinds) lies directly adjacent to joints.

Rinded, Intraformational Siltstone Clasts in Sandstone and Conglomerate

Two types of intraformational siltstone clasts are abundant above the erosional scours at the bases of sandstone bodies: 1) rinded concretions and 2) non-rinded ironstone. The rinded clasts (Figs. 1, 9) have densely cemented, iron-oxide rinds on their perimeters, and iron-poor, siltstone centers. They are most commonly tabular in cross section, but others are ovoid, or spindle shaped. In thin sections, the channel sandstone is in sharp contact with silt-size quartz grains that are enclosed within opaque iron-oxide cement. The outer edge of the iron-cemented rind coincides perfectly with the outer edge of the transported siltstone clasts. Silt-size quartz grains in the rinds are distributed in distinctive, circular patterns (Fig. 9C). Fractures that cut the rinded clasts (Fig. 9A) coincide with joints in outcrop. At Lost Spring Mountain, fractures in rinded concretions have a mean resultant direction of $152^{\circ}/332^{\circ}$ (Fig. 9D). Joints that traverse the rinded clasts (Fig. 9A) are enclosed by a double wall of iron oxide, one rind on each side of the fracture. Wedge-shaped, iron-cemented ridges with central fractures (Fig. 9B) protrude inward toward concretion interiors, and do not crosscut entire concretions. Millimeter-scale tubules cemented by iron oxide are abundant in joint-bounded compartments. These clasts are usually absent in strata that contain abundant coarse, siliciclastic pebbles.

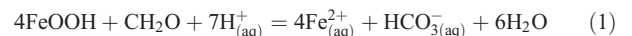
Non-Rinded Ironstone Clasts in Sandstone and Conglomerate

These clasts are siltstone and sandstone pebbles that are evenly cemented by iron oxide. They are present as lags at the bases of sandstone and conglomerates (Fig. 10). They are usually absent in conglomerates rich in cm-scale quartz pebbles. Some are rounded, but most are angular, and many of the angular clasts are curved in cross section.

INTERPRETATION OF IRON-RICH STRUCTURES

Discoidal Concretions

These concretions are products of anoxic conditions, as evidenced by the thin lamination in the host siltstone and the reduced-metal carbonate minerals that dominate their mineral constituents (Berner 1981; Burgess 2014). Cements formed early (Fig. 11), beneath heavily vegetated, marshy floodplains (cf. Aslan and Autin 1999), and displaced detrital grains as they grew in the shallow subsurface. Iron-reducing microbes oxidized buried organic matter and used ferric iron as an electron acceptor (Konhauser 2006) following a reaction similar to



Reduction of ferric iron minerals consumed acid and released of Fe^{++} and HCO_3^{-} to pore water, resulting in siderite precipitation. Multiple episodes of fracturing and fracture filling occurred with burial. The

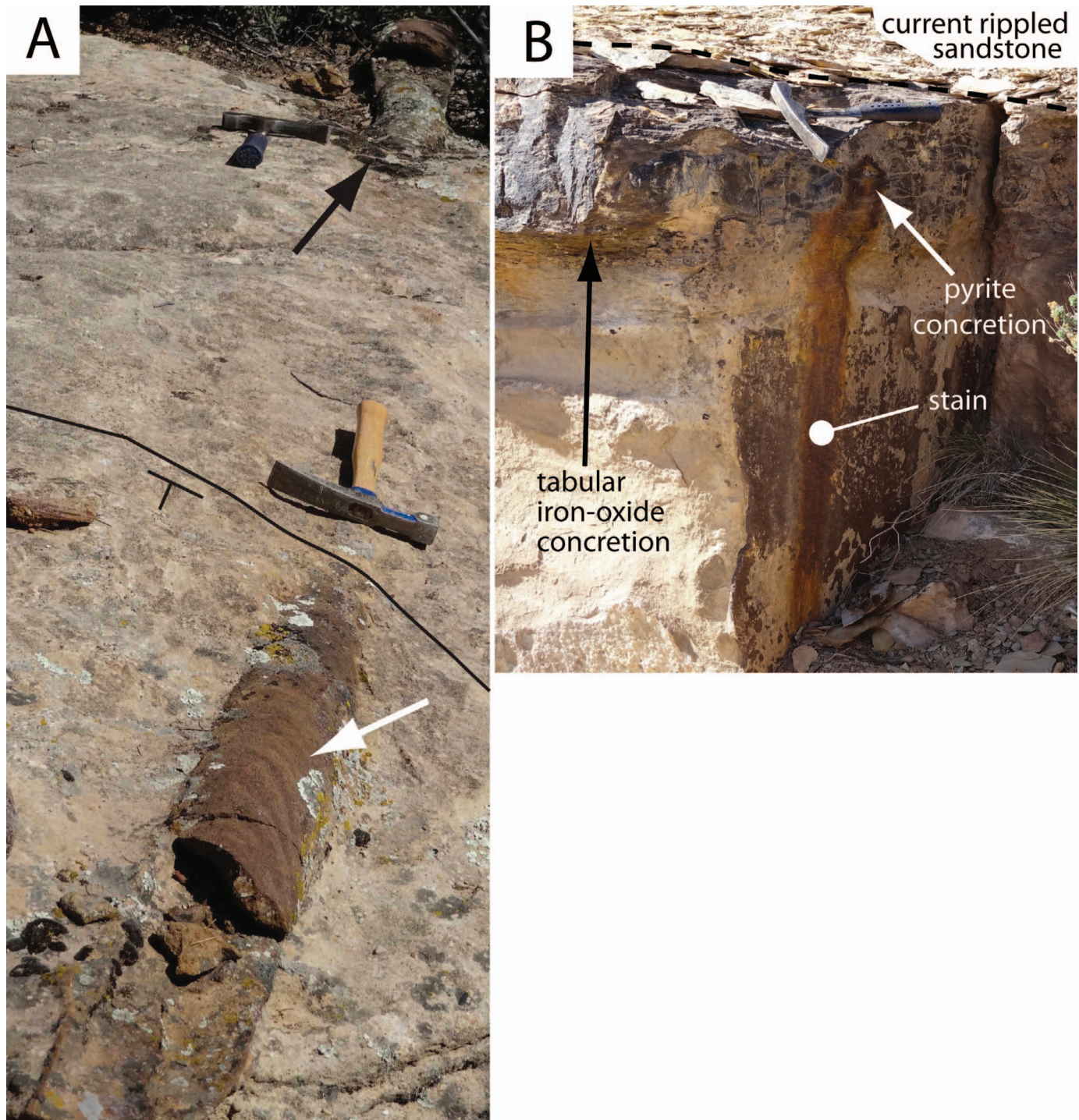


FIG. 6.—**A**) Cylindrical structure cemented by iron-oxide pseudomorphs after siderite. Cross-strata (white arrow) are directed down flow. Cylinder marks the former position of a large log that became oriented parallel to the fluvial paleoflow direction before being buried by trough cross-strata. Decomposition of the wood by methanogenic microbes raised the alkalinity of the surrounding pore water, causing precipitation of siderite. **B**) Pyrite and iron-oxide concretions at Little Creek Mountain. Contact between current-rippled sandstone and cross bedded sandstone marked by dashed line just above hammer. Pyrite concretion is still being oxidized in the vadose zone. Iron-oxide concretion is tabular and jointed; it formed via siderite oxidation.

iron-oxide dendrites record an oxidation event (Fig. 11) that progressed inward. The tiny fractures that cut dendrites likely formed during compaction, and suggest an early origin for the dendrites. This oxidation was probably a consequence of the falling Triassic water table during drought or local downcutting by channels. The imperme-

able, thinly laminated silt unit likely protected the bulk of the large concretions from oxidizing waters, allowing preservation of abundant siderite and rhodochrosite. In addition to the decimeter-scale, discoidal concretions, the Triassic floodplain mudstones also contained mm-scale, disseminated spheroidal siderite nodules. The evidence for this comes



FIG. 7.—Cross section of a block of wonderstone. No primary sedimentary structures are visible. Dark bands are cemented by iron oxide and are interpreted as the metabolic waste of colonies of iron-oxidizing microbes. Convex-outward bands show that microbes occupied redox boundaries that were shifting radially outward—fingers of oxidizing water were expanding into zones of reducing water where siderite was still stable. Iron-oxide staining (s) is interpreted as Liesegang bands and abiotic (Kettler et al. 2015). Lighter, bleached (b) zones were originally stained but were later bleached.

from the iron-oxide rinds that surround intraformational clasts (see below).

Pyrite Concretions

Like siderite, pyrite is indicative of reducing conditions. Pyrite grew prior to siderite precipitation and methanogenesis, while H_2S was still present in the pore water. These concretions are currently undergoing oxidation in the vadose zone (Fig. 6B).

Disseminated Iron-Oxide Rhombs

Witzke and Ludvigson (1994) and Ludvigson et al. (1996) reported rhomb-shaped crystals of siderite from drill cores from subsurface Dakota sand bodies in western Iowa. Loope et al. (2012) interpreted the iron-oxide rhombs from Dakota outcrops in eastern Nebraska as pseudomorphs after siderite. Rhombic pseudomorphs after siderite are also abundant in the core stones of giant iron-oxide concretions of the Navajo Sandstone in southern Utah (Loope et al. 2011). The dense, iron-oxide rhombs in the Shinarump (Fig. 5; Kettler et al. 2015) are pseudomorphs after siderite; the rhombs containing less iron oxide may be pseudomorphs after ankerite— $(CaFe)CO_3$.

The presence of early diagenetic siderite concretions in the mudstone suggests that the disseminated rhombic crystals in the channel sandstones (now represented by iron-oxide pseudomorphs) also formed during early diagenesis (Fig. 11). Gaining stream systems prevail during episodes with positive water budgets; groundwater recharge exceeds evapotranspiration in these settings and the water table slopes toward the channel (Fig. 12A). If the floodplain of the gaining stream contains heavily vegetated marshes, anaerobic metabolic activity by iron reducers and methanogens will release ferrous iron and bicarbonate into the pore waters of the organic-rich muds. These conditions likely generated pore waters (in both the muds and underlying channel sands) with P_{CO_2} values that exceeded equilibrium with atmospheric levels of carbon dioxide. In the modern Okavango Delta, saturation indices for siderite have been shown to increase with increasing alkalinity produced by CO_2 degassing (Mladenov et al. 2014).

The cylindrical structures in the channel sandstones (Fig. 6) formed when methanogens decomposed the cellulose and lignin in transported logs. This anaerobic metabolic activity raised the alkalinity of the surrounding, cross bedded sediment, causing the strongly localized precipitation of siderite.

Many more rhombic crystals of siderite formed in the channel sandstones than are preserved as pseudomorphs today. The original siderite crystals (represented by the preserved pseudomorphs) could have been oxidized *in situ* either in the Triassic depositional environment or much later, after uplift and exhumation of the Colorado Plateau (Fig. 11). Kettler et al. (2015) concluded that disseminated siderite crystals were the source of iron for development of the wonderstone patterns in the Shinarump. In the wonderstone case, the crystals dissolved completely when oxygenated, phreatic pore water moved through lithified sandstone (not uncemented channel sand). The released ferrous iron migrated a few centimeters laterally and before being precipitated to form wonderstone patterns (Kettler et al. 2015). The tabular, jointed concretions (described below) formed in a somewhat similar way

Wonderstone Pattern in Sandstone

Kettler et al. (2015) showed that the stained intervals that lie between cement bands fit the Jablczynski spacing law, and therefore represent Liesegang banding. In contrast, the spacing of the cement bands does not fit the law. They therefore concluded that wonderstone fabric comprises both biotic components (iron-oxide cement bands) and abiotic components (Liesegang). Thick arcuate bands mark previously stable boundaries where microbes controlled redox fronts in sideritic sandstone undergoing alteration. Liesegang intervals record brief episodes when, due to changing oxygen levels, microbes briefly lost control of the redox boundary. In these episodes, the boundary moved relatively rapidly down the oxygen gradient, toward the source of ferrous iron.

Type 1 patterns (Fig. 1) reflect the inward migration of redox boundaries (Kettler et al. 2015). Joint-defined sandstone blocks contained disseminated siderite crystals that formed during early diagenesis. Meteoric water carrying oxygen reached the perimeters of the blocks via the joints. As oxidation proceeded, the siderite crystals were dissolved and ferrous iron was oxidized to form ferric iron stain and cement.

The convex-outward (type 2) patterns (Fig. 7) reflect the outward migration of redox fronts from radially expanding conduits of oxygenated water that was flowing down gradient through the aquifer. Loope et al. (2011) used this explanation for similar structures in the Jurassic Navajo Sandstone.

Development of the wonderstone pattern requires a permeable, water-saturated matrix. Secondly, oxygen levels must be appropriate for iron-oxidizing microbes: in water that carries copious oxygen, abiotic processes

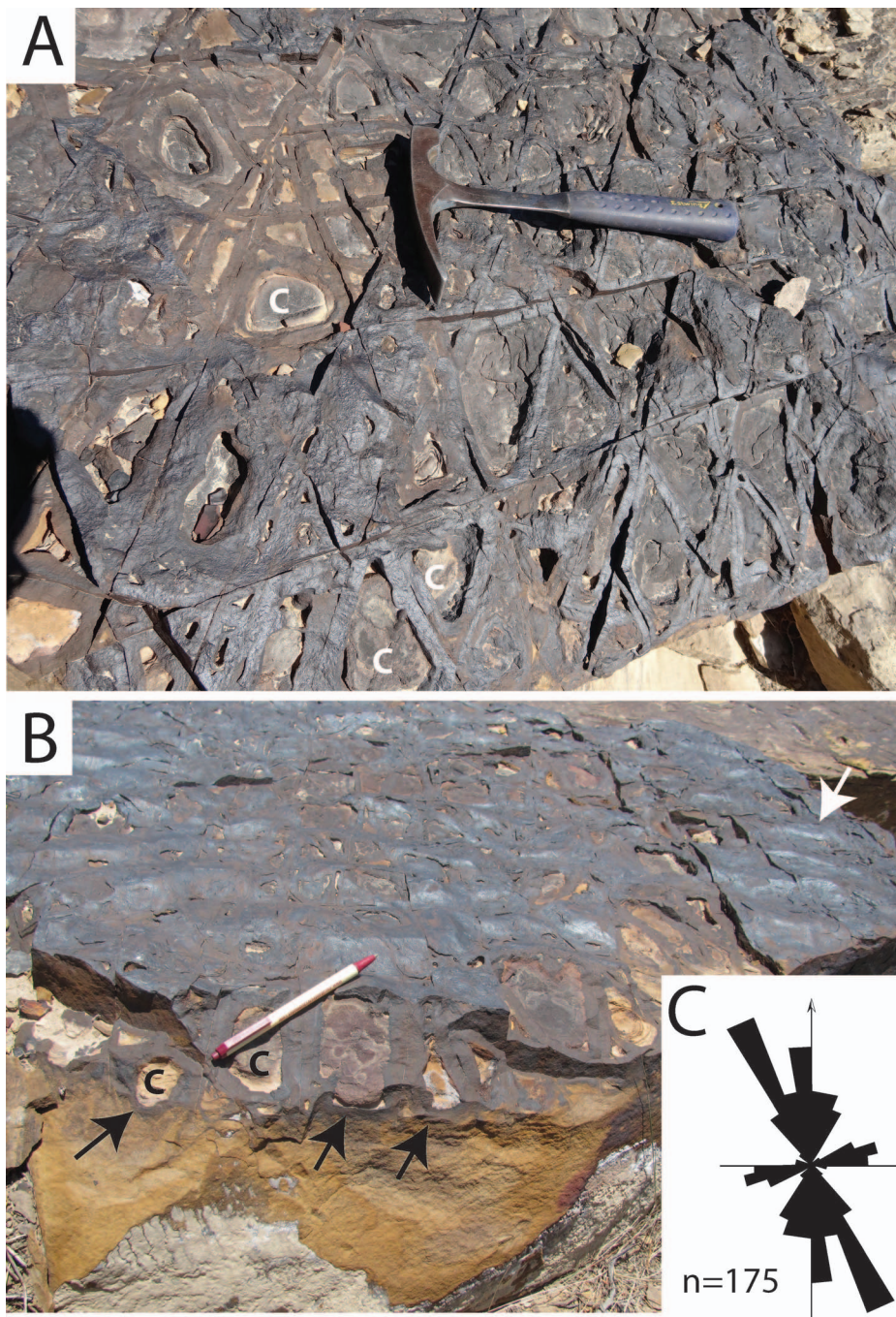


FIG. 8.—Tabular, jointed concretions in current-ripple-laminated sandstone at Little Creek Mountain. Overlying siltstone has been eroded away. **A)** Joints are bounded by sandstone that is heavily cemented by iron oxide; central cores (c) are iron-poor. Interpretation: top of the channel sand body was in contact with organic-rich siltstone. Siderite grew in the siltstone and underlying sand because metabolic activity of iron-reducing and methanogenic microbes raised the concentration of ferrous iron and the alkalinity of pore water, causing saturation for siderite. After sand became lithified, the sandstone was cut by joints. As Shinarump was exhumed, joints became conduits for oxygenated water. Microbes occupied rock adjacent to joints and mediated oxidation of siderite, forming thick rinds. **B)** Rippled upper surface (white arrow) is the contact with overlying siltstone. Note that iron-oxide rinds (black arrows) pass beneath cores (c), showing that siderite cement was most abundant in uppermost part of sandstone. **C)** Orientations of joints cutting tabular concretions, Little Creek Mountain.

can oxidize ferrous iron much more rapidly than can microbes, resulting in pseudomorphs, not wonderstone. Under microaerobic (< 200 mmol/l), near-neutral pH conditions, however, iron oxidation by *Gallionella ferruginea* is 60 times faster than the abiotic reactions (Sogaard et al. 2000; Konhauser et al. 2002), and wonderstone forms.

Disseminated siderite crystals were the source of both carbon and energy for the microbial colonies that generated wonderstone (Kettler et al. 2015). The ferric-iron cement bands are the wastes of these colonies. Some of the abundant siderite crystals were preserved as pseudomorphs, while others were dissolved completely to form wonderstone. Joint control of oxidation shows that wonderstone developed during Neogene exhumation of lithified Shinarump strata. The preserved iron-oxide pseudomorphs,

however, are products of oxygenation events that took place locally in the Triassic sedimentary environment (Fig. 11). The iron-oxidizing microbes imaged from wonderstone by Kettler et al. (2015) lived in lithified sandstones with much lower permeability than uncemented, uncompacted fluvial sand bodies. During Triassic arid intervals (Dubiel and Hasiotis 2011), the circulation of groundwater through (unlithified, uncompacted) channel sands may have reversed (Fig. 12B): river water and its dissolved oxygen (rather than reduced groundwater) would then have moved into buried sand bodies. Under such conditions, abiotic oxidation would likely have been more rapid than biotic oxidation, and iron oxide would have accumulated in pseudomorphs, rather than in the cement bands of wonderstone.

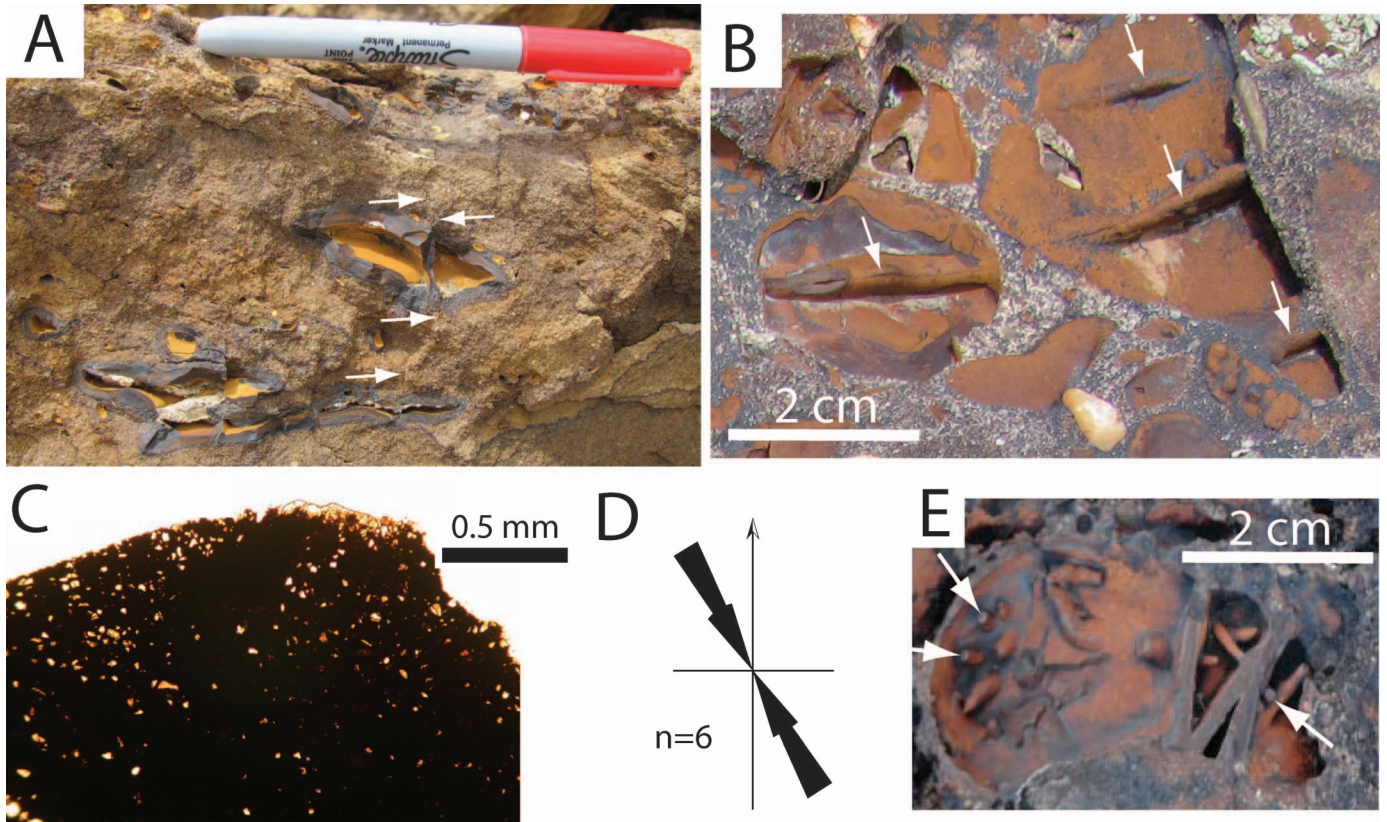


FIG. 9.—Rinded, intraformational siltstone clasts, Lost Spring Mountain. **A)** Vertical, cross-sectional view of two transported clasts in sandstone. White arrows mark a hairline fracture that cuts both clasts. In the clasts, iron oxide accumulated not only around clast perimeters but also on both sides of the hairline fracture, showing that oxidation followed formation of that fracture. **B)** Plan view of the interior of several transported clasts. Note that three iron-oxide-coated fractures (white arrows) in the largest clast lie parallel to one another and to a fourth fracture in the clast to the left. As in Part A, this shows that individual fractures connect adjacent clasts, and that fracturing preceded oxidation. **C)** Thin section of the rind from a rinded clast. Note the circular to oval zones with few silt-size quartz grains. This pattern formed via displacive, early growth of siderite nodules in floodplain siltstone and was preserved when ferrous iron migrated to the microbial colony at the perimeter of the transported clasts (cf. Ludvigson et al. 1998, their fig. 1; Loope et al. 2012, their fig. 3H). **D)** Orientations of fractures cutting rinded siltstone clasts (as in Part A). **E)** Iron-oxide tubules inside a rinded siltstone clast. Arrows point to transverse cross sections of tubules. Tubules are interpreted as channels made by Triassic roots that became conduits for oxygen during the Neogene.

Pyrite Concretions

Pyrite and siderite are commonly found together in organic-rich floodplain deposits. Iron sulfides (pyrite and its precursors) precipitate when available ferrous iron combines with H_2S produced by sulfate-reducing microbes. Siderite can precipitate only after the SO_4 is depleted. Although siderite oxidation has gone virtually to completion in the sandstone outcrops we studied, considerable pyrite oxidation is still taking place on these same outcrops (Fig. 6B).

Tabular, Jointed Concretions in Sandstones

These structures are the oxidized remains of laterally amalgamated, siderite-cemented concretions. The metabolic activity of anaerobic microbes raises the pH of pore waters (Konhauser 2006). Uptake of CO_2 by methanogens living in the organic-rich muds raised the pH of the pore waters in the adjacent sand, thereby triggering siderite precipitation in the underlying sandstone.

Although the diagenetic siderite accumulated in the Triassic depositional environment, accumulation of iron oxide along joints indicates that oxidation of this siderite postdated lithification of the host sandstone (Fig. 11).



FIG. 10.—Non-rinded intraformational clasts, vertical outcrop of lag deposit, Lost Spring Mountain. Note curved shape of several clasts (cf. Fig. 4B).

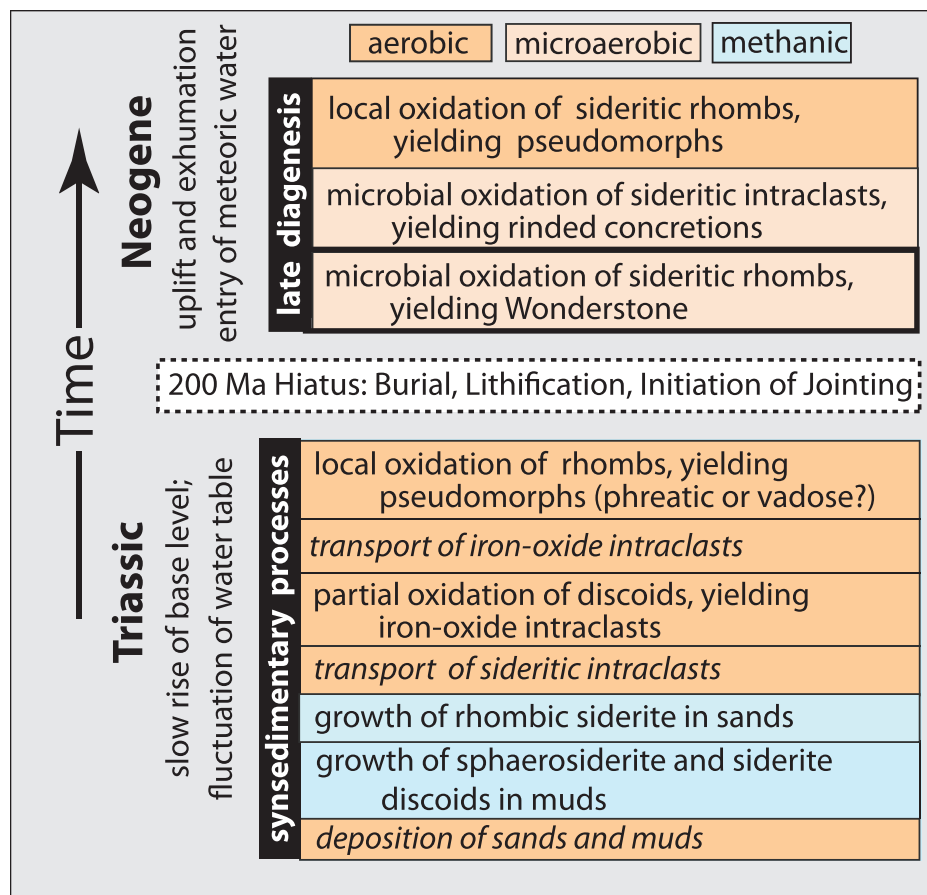


FIG. 11.—Sequence of depositional and diagenetic events, Shinarump Member.

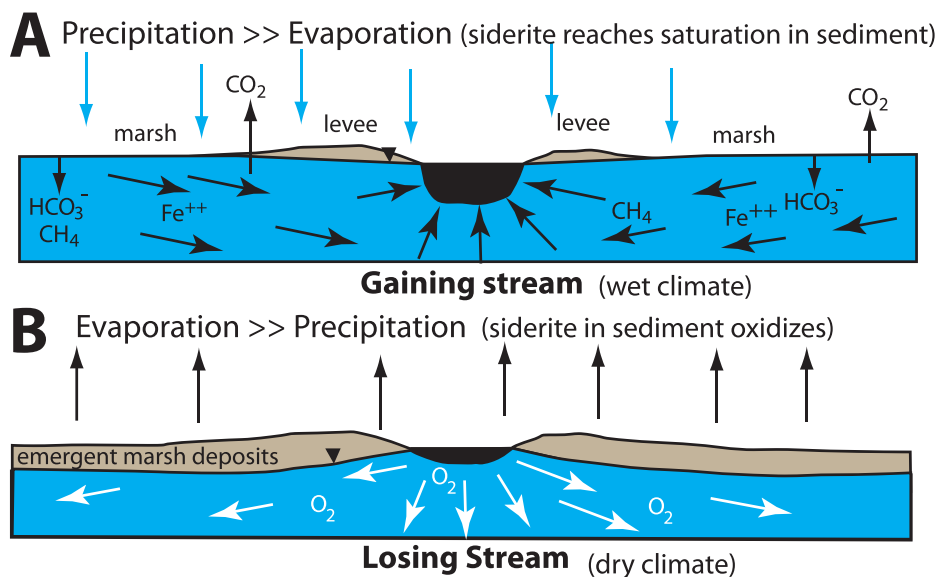


FIG. 12.—Hypothesis relating siderite growth and siderite oxidation to groundwater flow beneath streams. **A**) In a wet climate, the precipitation on the floodplain maintains a high water table that slopes toward the channel. Abundant vascular plants grow in adjacent, marshy habitats. Decomposition of organic matter by microbes leads to iron reduction and methane production. Reducing groundwater (black arrows) carrying ferrous iron and methane moves through marsh sediments and into underlying channel sands where siderite precipitates. Reducing water discharges to the active river channel. **B**) During dry climatic episodes, evaporation causes the groundwater table to drop. Because the water table now slopes away from the channel, the flow direction reverses. Oxygenated water in the channel (white arrows) moves rapidly into sand bodies, potentially oxidizing rhombic siderite abiotically. Dry episodes during the Triassic could thus explain how rhombic iron-oxide pseudomorphs were preserved. Otherwise, all of the rhombic siderite crystals could have been dissolved 200 million years later by the Neogene microbes that produced wonderstone at low oxygen concentrations in a less permeable, well-lithified sandstone.

Oxygenated waters moved preferentially along joints and eventually flushed reducing water from the aquifer. As in the box-work concretions in the Navajo Sandstone (Loope et al. 2011), ferrous iron from dissolving siderite in the sandstone diffused to redox boundaries that developed along the joints. Iron oxide was likely precipitated by iron-oxidizing microbial colonies (Kettler et al. 2015). Rinds progressively thickened as the redox boundary slowly migrated into the rock (toward the remaining siderite) and away from the joints. No rind formed along the upper surface of the tabular, siderite-cemented mass because the overlying, impermeable mudstone greatly diminished the oxygen supply. As this siderite dissolved, the ferrous iron was oxidized along the nearest joint.

The N- and NNW-dominated joint pattern shown in the Shinarump's tabular concretions at Little Creek Mountain is similar to the pattern displayed on a much larger scale in the Navajo Sandstone of Zion National Park, thirty kilometers to the northeast. In their analysis of the joints at Zion, Rogers et al. (2004) related the joints at Zion to the Miocene-to-Recent counterclockwise rotation of regional extensional stresses in the eastern Basin and Range province. Iron-oxide accumulations along these relatively young joints indicate that much (but not all) of the siderite that precipitated in the Triassic floodplain and channel sediments was preserved until the strata were lithified and exhumed (Fig. 11). Studies of the Hurricane Fault (Fig. 2) have shown that as the Basin and Range collapsed, the western Colorado Plateau (including the current study area) has been uplifted 1000 to 1500 m since the late Miocene (Anderson and Christenson 1989; Biek et al. 2003). Oxidizing meteoric waters invaded the joints during Neogene exhumation and oxidized 200-million-year-old siderite (Fig. 11).

Rinded, Intraformational Clasts

These clasts (Fig. 9) are directly analogous to the Pleistocene "rattle stones" described by Van der Burg (1969) and the Cretaceous rinded concretions of Loope et al. (2012). The circular patterns in the rinds (Fig. 9C) are evidence for displacive growth of siderite nodules in the floodplain silt (Ludvigson et al. 1998; Loope et al. 2012). Clasts composed of siderite-cemented silt entered the channel as it migrated across a vegetated floodplain, and became abraded during transport.

As with the box-like, tabular concretions, iron oxide accumulated along both sides of NNW-trending joints that cut the intraformational clasts. This indicates that oxidation of the siderite inside the siltstone clasts also took place after lithification, probably during the Neogene (Fig. 11). The small iron-oxide tubules (Fig. 9E) formed along root channels in the silt clasts became the conduits for oxygen.

Non-Rinded Ironstone Clasts

The non-rinded ironstone clasts are similar to the clasts derived from shattered discoidal concretions exposed on the modern outcrops of Shinarump siltstones (Fig. 4B). These clasts are the remains of discoidal concretions that formed in water-saturated, floodplain muds but were oxidized in the Shinarump depositional setting when the groundwater table dropped during droughts or as a consequence of deep channel incision.

In their study of the basal Shinarump Member and the uppermost beds of the underlying Moenkopi Formation, Dubiel and Hasiotis (2011) found deep (up to 3 m), vertical crayfish burrows penetrating pedogenic ironstone. The burrows are filled with iron-poor sediment. They attributed the deep excavations to a long-persisting drop in the groundwater table during Shinarump deposition. The interpretation that some discoids and rhombic crystals were oxidized during the Triassic (Fig. 11) is consistent with groundwater declines of lesser duration.

DISCUSSION

Shinarump channel sandstones demonstrate that disseminated crystals of reduced-iron minerals in a porous and permeable matrix are the precursors of wonderstone—the complex pattern of iron-oxide cementation and stains that were the motivation for this study. Fluvial channel deposits that are juxtaposed against floodplain deposits rich in decomposing vascular plants (Shinarump and Dakota) can develop these patterns, but they are not unique in this regard. Although little, if any coal deposits accumulated, it is apparent that the poorly drained Shinarump floodplains were sites of dense plant growth. Wonderstone patterns can also develop, however, in other sedimentary systems. Siderite can be a late diagenetic product in eolian sandstones (Navajo Sandstone; Loope et al. 2011) and in pre-Silurian fluvial sandstones (Umm Ishrin Formation; Loope et al. 2010; Kettler et al. 2015). In all of these examples of wonderstone, iron was originally present as iron-oxide coatings on clastic particles; the migration of methanic, reducing waters allowed the dissolution of the grain coating oxides and the growth of siderite crystals in the sediment with relatively low organic content.

Heterotrophic, iron-reducing microbes metabolized buried organic matter in the floodplain mud and used the ferric iron in grain coatings as their electron acceptor (Konhauser 2006). The ferrous iron they released was the source of iron for siderite precipitation. The eventual dissolution of disseminated siderite crystals provided the energy source for the iron-oxidizing microbes that mediated the oxidation process. Ferric iron in the wonderstone cement represents the wastes of these micro-aerobic colonies (Weber et al. 2012; Kettler et al. 2015). Heavy accumulations of iron oxide cement along joints indicate that the Wonderstone fabric is late diagenetic—it did not develop until Neogene uplift and exhumation of the Colorado Plateau allowed influx of oxygenated meteoric water into the lithified strata.

The iron-oxide accumulations in the Shinarump Member of the Chinle Formation provide clues to the unit's depositional and diagenetic history (Fig. 11), but also reflect the region's tectonic and geomorphic evolution. With Colorado Plateau uplift and exhumation, the sandstones of the Grand Staircase were drained of groundwater as the cliffs migrated northward. Along the Shinarump Cliffs (Fig. 2), north-dipping outcrops of wonderstone are directly up-dip from Shinarump sandstones in the shallow subsurface that are in contact with overlying Quaternary alluvium (Fig. 13). Those subsurface rocks are likely saturated with oxidizing groundwater, and wonderstone could be actively forming there. Pore waters in the rock in direct contact with the alluvium may contain too much O₂ for establishment of microaerobic iron-oxidizers, but O₂ levels down-dip from this contact may be appropriate for their activity. If siderite is being metabolized in this zone, the iron-oxide cements in the nearby, outcropping wonderstone may be only tens of thousands to hundreds of thousands of years old.

Although siderite is known to be abundant in Recent methanic floodplain sediments (Ho and Coleman 1969; Aslan and Autin 1999; also see summary in Ludvigson et al. 2013), extensive siderite cements have not been documented in Recent channel sands. The rock record provides circumstantial evidence that abundant disseminated siderite can form in channel sandstones penecontemporaneously with the siderite in adjacent floodplains. Close inspection of shallow cores retrieved from active meander belts could confirm this hypothesis.

CONCLUSIONS

1. Both early-diagenetic pyrite and siderite were present in the Shinarump Member of the Chinle Formation, but siderite was dominant. Siderite is the principal early, iron-bearing diagenetic phase in modern fluvial sedimentary systems, but unlike pyrite, it rarely survives contact with oxidizing groundwater.

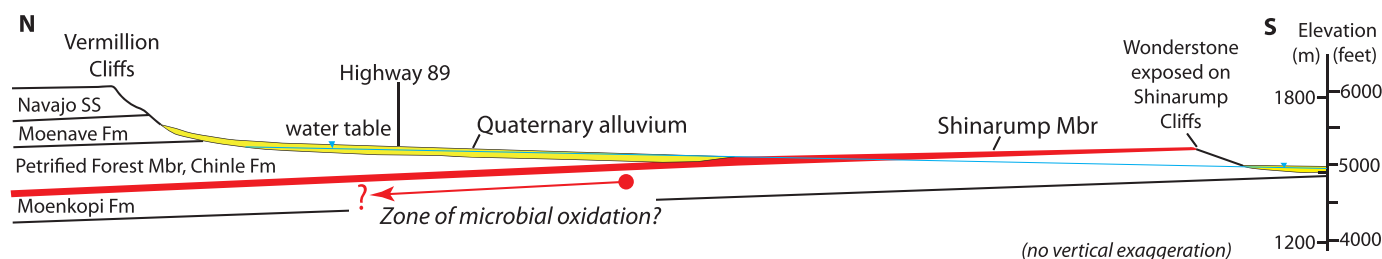


FIG. 13.—North–south cross section of Mesozoic strata east of Kanab, Utah showing a zone where Shinarump sandstone is likely saturated by oxygenated water in the shallow subsurface. Iron-oxidizing microbes living in this zone may be metabolizing siderite and generating the wonderstone pattern. Modified from a cross section in Hayden (2011).

2. *In situ* discoidal concretions and reworked, iron-rich mud balls provide evidence of early accumulation of siderite in Shinarump floodplain siltstone.
3. Rhombic, iron-oxide pseudomorphs show that siderite also formed in channel sandstones. Many of these rhombic crystals were dissolved during late-stage diagenesis, and the ferrous iron was used by iron-oxidizing microbes as an energy source. The bands of iron-oxide cement that form wonderstone represent the metabolic waste of microbial communities. Siderite crystals that were not metabolized were oxidized abiotically, and are now preserved as pseudomorphs.
4. Iron-oxide cement bands in wonderstone are convex in the direction of oxygen migration and form two distinct patterns: 1) progressive inward movement of O_2 from bounding joints into isolated blocks; and 2) radial, outward migration of O_2 from the most permeable pathways in the aquifer.
5. Wonderstone in Shinarump sandstones started to form during the Neogene as the Colorado Plateau was exhumed; it is likely still forming today in the shallow subsurface.

ACKNOWLEDGMENTS

We thank Ken Brown (Western Hills Rock & Gems, Kanab, Utah) and Rody Cox (Bureau of Land Management, St. George, Utah) for their helpful suggestions and cooperation. The NASA Nebraska Space Grant program and the UNL Vice-Chancellor for Research provided funding for this research. We also acknowledge the National Geographic Society (Committee for Research and Exploration Grant #9255-13) for support of a parallel project carried out in Jordan that yielded invaluable insights applicable to this work. Helpful suggestions by Marsha French, Joann Welton, Leslie Melim, John Southard, and an anonymous reviewer greatly improved the manuscript.

REFERENCES

- ANDERSON, R.E., AND CHRISTIANSON, G.E., 1989, Quaternary faults, folds, and selected volcanic features in the Cedar City $1^\circ \times 2^\circ$ quadrangle, Utah: Utah Geological and Mineralogical Survey, Miscellaneous Publication 89-6, scale 1:250,000, 29 p.
- ASLAN, A., AND AUTIN, W.J., 1999, Evolution of the Holocene Mississippi River floodplain, Ferriday, Louisiana: insights on the origin of fine-grained floodplains: *Journal of Sedimentary Research*, v. 69, p. 800–815.
- ATCHLEY, S.C., NORDT, L.C., DWORKIN, S.I., RAMEZANI, J., PARKER, W.G., ASH, S.R., AND BOWRING, S.A., 2013, A linkage among Pangean tectonism, cyclic alluviation, climate change, and biologic turnover in the Late Triassic: the record from the Chinle Formation, southwestern United States: *Journal of Sedimentary Research*, v. 81, p. 1147–1161.
- BEER, J.J., 2005, Sequence stratigraphy of fluvial and lacustrine deposits in the lower part of the Chinle Formation, south central Utah, United States: paleoclimatic and tectonic implications [Unpublished M.S. thesis]: University of Minnesota–Duluth, 169 p.
- BEITLER, B., CHAN, M.A., AND PARRY, W.T., 2003, Bleaching of Jurassic Navajo Sandstone on Colorado Plateau Laramide highs: evidence of exhumed hydrocarbon supergiants?: *Geology*, v. 31, p. 1041–1044.
- BERNER, R.A., 1981, A new geochemical classification of sedimentary environments: *Journal of Sedimentary Petrology*, v. 51, p. 359–365.
- BIEK, R.F., WILLIS, G.C., HYLLAND, M.D., AND DOELLING, H.H., 2003, *Geology of Zion National Park, Utah*, in Sprinkel, D.A., Chidsey, T.C., and Anderson, P.B., eds., *Geology of Utah's Parks and Monuments: Utah Geological Association, Publication 28*, p. 107–135.
- BLAKE, R.C., AND GUBITOSA, R., 1983, Late Triassic paleogeography and depositional history of the Chinle Formation, southeastern Utah and northern Arizona, in Reynolds, R.M., and Dolly, E.D., eds., *Mesozoic Paleogeography of West-Central United States: SEPM, Rocky Mountain Section*, p. 57–76.
- BURGESS, D.T., 2014, Early and Late Iron Diagenesis in the Upper Triassic Shinarump Member of the Chinle Formation (Utah and Arizona) [Unpublished M.S. thesis]: University of Nebraska–Lincoln, 64 p.
- CURTIS, C.D., AND COLEMAN, M.L., 1986, Controls on the precipitation of early diagenetic calcite, dolomite, and siderite concretions in complex depositional sequences, in Gautier, D.L., ed., *Roles of Organic Matter in Sediment Diagenesis: SEPM, Special Publication 38*, p. 23–33.
- DICKINSON, W.R., 1981, Plate tectonic evolution of the southern Cordillera, in Dickinson, W.R., and Payne, W.D., eds., *Relations of Tectonics to Ore Deposits in the Southern Cordillera: Arizona Geological Society, Digest*, v. 14, p. 113–135.
- DICKINSON, W.R., AND GEHRELS, G.E., 2008, U-PB Ages of detrital zircons in relation to paleogeography: Triassic paleodrainage networks and sediment dispersal across southwest Laurentia: *Journal of Sedimentary Research*, v. 78, p. 745–764.
- DUBIEL, R.F., 1992, Architectural facies analysis of non-marine depositional systems in the Upper Triassic Chinle Formation, southeastern Utah, in Miall, A.D., and Tyler, N., eds., *The Three Dimensional Architecture of Terrigenous Clastic Sediments and Its Implications for Hydrocarbon Discovery and Recovery: SEPM, Concepts in Sedimentology and Paleontology*, v. 3, p. 104–110.
- DUBIEL, R.F., AND HASIOTIS, S.T., 2011, Deposystems, paleosols, and climatic variability in a continental system: the upper Triassic Chinle Formation, Colorado Plateau, U.S.A., in Davidson, S.K., Leleu, S., and North, C.P., eds., *The Preservation of Fluvial Sediments and Their Subsequent Interpretation: SEPM, Special Publication 97*, p. 393–421.
- HAYDEN, J.M., 2011, Geologic map of the Thompson Point Quadrangle, Kane County, Utah, and Coconino County, Arizona: Utah Geological Survey, Map 249DM.
- HAZEN, R.M., PAPINEAU, D., BLEEKER, W., DOWNS, R.T., FERRY, J.M., MCCOY, T.J., SVERJENSKY, D.A., AND YANG, H., 2008, Mineral evolution: *American Mineralogist*, v. 93, p. 1693–1720.
- HO, C., AND COLEMAN, J.M., 1969, Consolidation and cementation of recent sediments in the Atchafalaya basin: *Geological Society of America, Bulletin*, v. 80, p. 183–192.
- KETTLER, R.M., LOOPE, D.B., AND WEBER, K.A., 2011, Follow the water: Connecting a CO_2 reservoir and bleached sandstone to iron-rich concretions in the Navajo Sandstone of south-central Utah: Reply to Comment: *Geology*, v. 39, p. E251–E252.
- KETTLER, R.M., LOOPE, D.B., WEBER, K.A., AND NILES, P.B., 2015, Life and Liesegang: outcrop-scale microbially induced diagenetic structures and geochemical self-organization phenomena produced by oxidation of reduced iron: *Astrobiology*, v. 15, p. 616–636.
- KONHAUSER, K.O., 2006, *Introduction to Geomicrobiology: Malden, Massachusetts: Blackwell Publishing*, 425 p.
- KONHAUSER, K.O., HAMADE, T., RAISWELL, R., MORRIS, R.C., FERRIS, F.G., SOUTHAM, G., AND CANFIELD, D.E., 2002, Could bacteria have formed the Precambrian banded iron formations: *Geology*, v. 30, p. 1079–1082.
- LOOPE, D.B., AND KETTLER, R.M., 2015, The footprints of ancient CO_2 -driven flow systems: ferrous carbonate concretions below bleached sandstone: *Geosphere*, v. 11, p. 943–957.
- LOOPE, D.B., KETTLER, R.M., AND WEBER, K.A., 2010, Follow the water: connecting a CO_2 reservoir and bleached sandstone to iron-rich concretions in the Navajo Sandstone of south-central Utah, USA: *Geology*, v. 38, p. 999–1002.
- LOOPE, D.B., KETTLER, R.M., AND WEBER, K.A., 2011, Morphologic clues to the origins of iron oxide-cemented spheroids, boxworks, and pipelike concretions, Navajo Sandstone of South-Central Utah, U.S.A.: *Journal of Geology*, v. 119, p. 505–520.
- LOOPE, D.B., KETTLER, R.M., WEBER, K.A., HINRICH, N.L., AND BURGESS, D.T., 2012, Rinded iron-oxide concretions: hallmarks of altered siderite masses of both early and late diagenetic origin: *Sedimentology*, v. 59, p. 1769–1781.
- LUDVIGSON, G.A., AND RAVN, R.L., 1996, New insights on the sequence stratigraphic architecture of the Dakota Formation in Kansas–Nebraska–Iowa from a decade of sponsored research activity: *Current Research in Earth Sciences, Bulletin 258*, p. 1039–1042.

- LUDVIGSON, G.A., GONZALEZ, L.A., WITZKE, B.J., BRENNER, R.L., AND METZGER, R.A., 1996, Diagenesis of iron minerals in the Dakota Formation, *in* Witzke, B.J., and Ludvigson, G.A., eds., *Mid-Cretaceous Fluvial Deposits of the Eastern Margin, Western Interior Basin: Nishnabotna Member, Dakota Formation: Iowa Department of Natural Resources, Geological Survey Bureau, Guidebook Series*, v. 17, p. 31–38.
- LUDVIGSON, G.A., GONZALEZ, L.A., METZGER, R.A., WITZKE, B.J., BRENNER, R.L., MURILLO, A.P., AND WHITE, T.S., 1998, Meteoric sphaerosiderite lines and their use for paleohydrology and paleoclimatology: *Geology*, v. 26, p. 1039–1042.
- LUDVIGSON, G.A., FOWLE, D.A., ROBERTS, J.A., GONZÁLEZ, L.A., DRIESE, S.G., PLACE, O.B., VILLARREAL, M.A., SMITH, J.J., AND SUAREZ, M.B., 2013, Paleoclimatic applications and modern process studies of pedogenic siderite, *in* Driese, S.G., and Nordt, L.C., eds., *New Frontiers in Paleopedology and Terrestrial Paleoclimatology: SEPM, Special Publication 104*, p. 79–87.
- MLADENOV, N., WOLSKI, P., HETTIARACHCHI, G.M., MURRAY-HUDSON, M., ENRIQUEZ, H., DAMARAJU, S., GALKADUWA, M.B., MCKNIGHT, D.M., AND MASAMBA, W., 2014, Abiotic and biotic factors influencing the mobility of arsenic in groundwater of a through-flow island in the Okavango Delta, Botswana: *Journal of Hydrology*, v. 518, p. 326–341.
- PROCHNOW, S.J., NORDT, L.C., ATCHLEY, S.C., AND HUDEC, M.R., 2006, Multi-proxy paleosol evidence for Middle and Late Triassic climate trends in eastern Utah: *Palaeogeography, Palaeoclimatology, Palaeoecology*, v. 232, p. 53–72.
- PYE, K., DICKSON, J.A.D., SCHIAVON, N., COLEMAN, M.L., AND COX, M., 1990, Formation of Siderite–Mg–calcite–iron sulphide concretions in intertidal marsh and sandflat sediments, north Norfolk, England: *Sedimentology*, v. 37, p. 325–343.
- ROGERS, C.M., DOUGLAS, A.M., AND ENGELDER, T., 2004 Kinematic implications of joint zones and isolated joints in the Navajo Sandstone at Zion National Park, Utah: Evidence for Cordilleran relaxation: *Tectonics*, v. 23, TC1007, doi: 10.1029/2001TC001329.
- SOGAARD, E.G., MEDENWALDT, R., AND ABRAHAM-PESKIR, J.V., 2000, Conditions and rates of biotic and abiotic iron precipitation in selected Danish fresh water plants and microscopic analysis of precipitate morphology: *Water Research*, v. 34, p. 2675–2682.
- STEWART, J.H., POOLE, F.G., AND WILSON, R.F., 1972, Stratigraphy and origin of the Chinle Formation and related Upper Triassic strata in the Colorado Plateau region: U.S. Geological Survey, Professional Paper 690, 336 p.
- VAN DER BURG, W.J., 1969, The formation of rattle stones and the climatological factors which limited their distribution in the Dutch Pleistocene, 1. The formation of rattle stones: *Paleogeography, Paleoclimatology, Paleocology*, v. 6, p. 105–124.
- VAN DER BURG, W.J., 1970, The formation of rattle stones and the climatological factors which limited their distribution in the Dutch Pleistocene, 2. The climatological factors: *Palaeogeography, Palaeoclimatology, Palaeoecology*, v. 6, p. 297–308.
- WALKER, T.R., 1974, Formation of red beds in moist tropical climates: a hypothesis: *Geological Society of America, Bulletin*, v. 85, p. 633–638.
- WALKER, T.R., WAUGH, B., AND CRONE, A.J., 1978, Diagenesis in first-cycle desert alluvium of Cenozoic age, southwestern United States and northwestern Mexico: *Geological Society of America, Bulletin*, v. 89, p. 19–32.
- WEBER, K.A., SPANBAUER, T.L., WACEY, D., KILBURN, M.R., LOOPE, D.B., AND KETTLER, R.M., 2012, Biosignatures link microorganisms to iron mineralization in a paleoquifer: *Geology*, v. 40, p. 747–750.
- WITZKE, B.J., AND LUDVIGSON, G.A., 1994, The Dakota Formation in Iowa and the type area, *in* Shurt, G.W., Ludvigson, G.A., and Hammond, R.H., eds., *Perspectives on the Eastern Margin of the Cretaceous Western Interior Basin: Geological Society of America, Special Paper 287*, p. 43–78.

Received 22 October 2015; accepted 13 February 2016.